Fault Diagnosis of Motor Drives Using Stator Current Signal Analysis Based on Dynamic Time Warping

D. Zhen[1*], T. Wang[2], F. Gu[1], and A. D. Ball[1]
[1]Centre for Diagnostic Engineering, University of Huddersfield, HD1 3DH, UK
[2]Department of Vehicle Engineering, Taiyuan University of Technology, 030024 Shanxi, P.R. China

ABSTRACT

Electrical motor stator current signals have been widely used to monitor the condition of induction machines and their downstream mechanical equipment. The key technique used for current signal analysis is based on Fourier transform (FT) to extract weak fault sideband components from signals predominated with supply frequency component and its higher order harmonics. However, the FT based method has limitations such as spectral leakage and aliasing, leading to significant errors in estimating the sideband components. Therefore, this paper presents the use of dynamic time warping (DTW) to process the motor current signals for detecting and quantifying common faults in a downstream two-stage reciprocating compressor. DTW is a time domain based method and its algorithm is simple and easy to be embedded into real-time devices. In this study DTW is used to suppress the supply frequency component and highlight the sideband components based on the introduction of a reference signal which has the same frequency components with the supply power. Moreover, a sliding window is designed to process the raw signal using DTW frame by frame for effective calculation. Based on the proposed method, the stator current signals measured from the compressor induced with different common faults and under different loads are analysed for fault diagnosis. Results show that DTW based on residual signal analysis through the introduction of a reference signal, allows the supply components to be suppressed well so that the fault related sideband components are highlighted for obtaining accurate fault detection and diagnosis results. In particular, the root mean square (RMS) values of the residual signal can indicate the differences between the healthy case and different faults under varying discharge pressures. It provides an effective and easy approach to the analysis of motor current signals for better fault diagnosis of the downstream mechanical equipment of motor drives in the time domain in comparison with conventional FT based methods.

Key word: Reciprocating Compressor, Dynamic Time Warping, Motor Current Signal.

1. Introduction

Electrical motor current signals have been widely investigated to analyse the health of the induction machine and their downstream mechanical equipment. [1, 2]. Moreover, because it is cost-effective in obtaining signals and allows remote monitoring, the induction machine stator current signal is also used to detect the influence of mechanical problems that result in rotor disturbances [1], and the presence of load imbalance can also be detected through analysing the induction machine stator current signals [3]. Recent studies [4] have shown that the supply currents can contain components related to abnormalities in downstream equipment such as compressors, pumps, rolling mills, mixers, crushers, fans, blowers and material conveyors and the technique has been used to detect specific axial flow compressor problems.

*Corresponding author. Tel.: +44 01484 473548/2965

E-mail address: D.Zhen@hud.ac.uk

Common approaches used for fault detection are based on the comparison of correlate numerical models with measured modal properties from undamaged and damaged components. Measurements are normally made in the time domain while a machine runs under different loads and speeds. Then the signals acquired in the test are analysed in both the time and the frequency domains using various signal processing techniques for extracting effective diagnostic features which allows accurate comparison between the signals.

Unfortunately, the signal processing techniques used for feature extraction are developed predominately in the frequency domain through Fourier transform (FT). Although it produces satisfactory results, the FT based method is subject to a number of generic limitations: aliasing [5], spectral leakage [6, 7] and picket-fence effect [5, 8]. Especially the latter two often lead to significant errors in spectrum estimation so that the weak signature due to faults in signals cannot be resolved properly for accurate fault detection and diagnosis. Although many methods have been developed to improve the limitations [5-8], they have never eliminated them completely. In addition, the computation complexity is also high which limits its application in real-time condition monitoring.

Thus it seems that techniques applied directly to the time domain signals can avoid the shortcomings of the frequency analysis. In fact, time domain based methods, especially time synchronous average (TSA) [9], have received intensive investigation in recent years for monitoring rotating machines and have gained many successful applications. However, it needs a shaft mark signal from an additional channel to implement TSA based monitoring, which leads to increased cost to applications. The statistical parameters or characteristic features can be calculated from time signals, such as mean, peak, standard deviation, root mean square (RMS), and kurtosis, etc. These features are very significant in obtaining accurate analysis results in the time domain. In some applications, such as speech recognition [10], signature matching [11] and condition monitoring [12], the common task with time series data is comparing one sequence with another in order to detect the differences between the two sequences for further analysis. However, it is often the case that two signals in the time domain have the similar overall component shapes [13], but out of synchronization and generally not of exactly the same length as shown in Figure 1(a). In order to find the exact dissimilarity between such two signals and as a pre-processing step before comparing them, it is necessary to match them to achieve an appropriate alignment.

Dynamic time warping (DTW) is an algorithm for aligning two such time series. The underlying principle behind DTW is, given two time series, to stretch or compress them locally in order to make one resemble the other as much as possible. The distance between them is computed, after stretching, by summing the distances of individual aligned elements (Figure 2). Figure 1(b) shows the alignment of the two time series processed by DTW.

The DTW is a popular algorithm applied in many areas. Bellman and Kalaba [14] first introduced it on adaptive control processes. It was popularised in the '70s, when it was mainly applied to isolated word recognition and speech recognition [11, 15-17] to account for differences in speaking rates between speakers and utterances. Since then, it has been employed for clustering and classification in countless domains: electro-cardiogram analysis [18-20], clustering of gene expression profiles [21, 22], biometrics [23, 24], process monitoring [25]. Moreover, DTW has been also used in handwriting and online signature matching [10], sign language recognition and gesture recognition, data mining and time series clustering, computer vision and computer animation, surveillance, protein sequence alignment and chemical engineering, music and signal processing [26]. Recently, Zhen D. et al [12, 27] have explored it in processing data from motors for condition monitoring and shown promising results in that the aligned signals by DTW do not lose information and is suitable for fault diagnosis. DTW can be used to suppress the supply frequency component and highlight the sideband components.

The rest of the paper will be organised as follows. In section 2, the DTW algorithm is reviewed to gain an understanding of DTW. Section 3 introduces the characteristics of electrical motor stator current signal. Subsequently, the proposed method for fault detection using DTW based on a sliding window is presented in section 4. Next, section 5 presents the experimental evaluation and result discussion. Section 6 gives the conclusions.

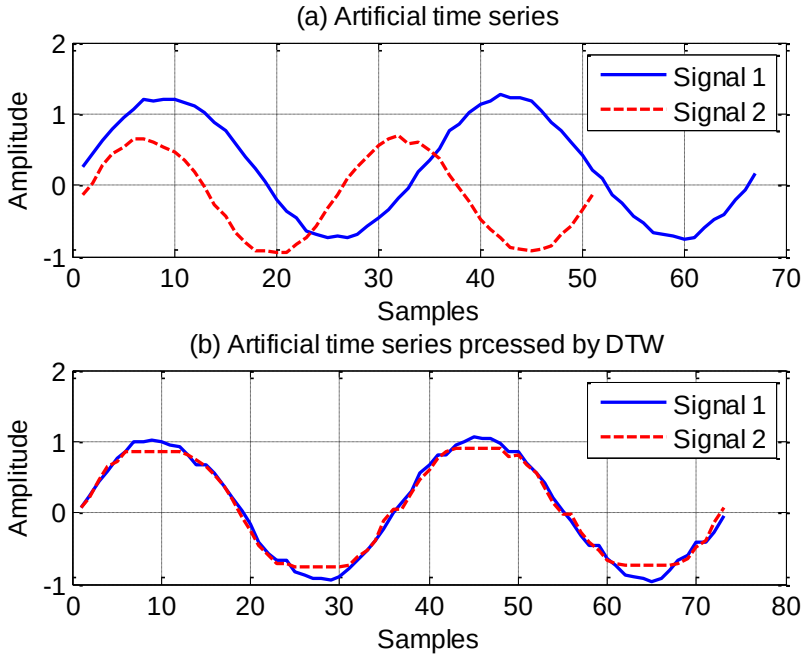

Figure 1 Time series aligned by DTW

2. Dynamic Time Warping

Given two time series of length N and M respectively.

$$X = (x_1, x_2, \cdots, x_N) \tag{1}$$

$$Y = (y_1, y_2, \cdots, y_M) \tag{2}$$

where x_i and y_j are represented by the sequences of values at the point i and j in the series X and Y respectively.

To align the two time series for comparison, a $\mathrm{N} \times \mathrm{M}$ distance matrix C is built firstly. The element of the matrix C is the distance between the two points $\mathrm{x_i}$ and $\mathrm{y_j}$ which is represented by $\mathrm{c_{ij}}$. Typically, the Euclidean distance is used to calculate the point-to-point distance by

$$\mathrm{c_{ij}} = (\mathrm{x_i} - \mathrm{y_j})^2 \tag{3}$$

Once the distance matrix has been built, the DTW algorithm finds the alignment path which runs through the matrix elements that defines a mapping between X and Y. The alignment path found by DTW is a warping path function which can be defined as:

$$W = (w_1, w_2, \cdots, w_K) \text{ With } w_k = (n_k, m_k) \tag{4}$$

Where

$n_k, = 1,2, \cdots, N; m_k = 1,2, \cdots, M; and\ k = 1,2, \cdots, K;$

In order to obtain the optimal alignment path, the DTW algorithm needs to be applied under certain conditions [13, 26]:

1. Boundary condition: $w_1 = (1, 1)$, and $w_K = (N, M)$. The starting and ending points of the warping path must be the first and the last points of aligned time series.
2. Monotonicity condition: Given $w_k = (n_k, m_k)$ then $w_{k-1} = (n_{k-1}, m_{k-1})$, where $n_{k,} - n_{k-1} \geq 0$ and $m_{k,} - m_{k-1} \geq 0$. This forces the points in W to be monotonically spaced in time.
3. Step size condition: Given $w_k = (n_k, m_k)$ then $w_{k-1} = (n_{k-1}, m_{k-1})$, where $n_{k,} - n_{k-1} \leq 1$ and $m_{k,} - m_{k-1} \leq 1$. The basic step size condition formulated as $w_k - w_{k-1} \in \{(1,1), (1,0), (0,1)\}$. This criterion limits the warping path from long jumps while aligning sequences, and restricts the allowable steps in the warping path to adjacent cells.

Noting that there is a large number of possible monotonically alignment paths increasing from $(1,1)$ to (N, M) according to the three certain conditions. Therefore a dynamic programming algorithm is introduced to test the length of all possible distortion paths and to determine the shortest one. The dynamic programming employs the cumulated distance $d_w(X,Y)$ between X and Y for a given warping path w, $d_w(X,Y)$ is the sum of the point-to-point distances c_{ij} along the warping path w.

$$d_w(X,Y) = \sum_{(i,j)\in w} c_{ij} \tag{5}$$

Noting that $w \in W = (w_1, w_2, \cdots, w_K)$ is the set of all possible warping paths. The goal of the dynamic programming is to determine an optimal warping path for which the cumulated distance between X and Y is minimal:

$$d^*(X,Y) = min_{w\in W}\, d_w(X,Y) \tag{6}$$

The optimal warping path is selected based on the cumulated matrix. Figure 2 is an example of optimal warping path selection based on a cumulated matrix for the two signals alignment which is shown in Figure 1(b). Assuming that the cumulative distance matrix is D, the $\mathrm{D}(\mathrm{i},\mathrm{j})$ are the elements of the cumulative distance matrix D which is defined as follows [27]:

1. First row: $D(1,j) = \sum_{k=1}^{j} c_{1k}, j \in [1{:}\,M]$.
2. First column: $D(i,1) = \sum_{k=1}^{i} c_{k1}, i \in [1{:}\,N]$.
3. All other elements:
$$D(i,j) = c_{ij} + min\{c_{i-1,j-1}, c_{i-1,j}, c_{i,j-1}\}, i \in [1{:}\,N], j \in [1{:}\,M] \tag{7}$$

Once the cumulated distance matrix is built, the alignment warping path could be found by the simple backtracking from the point $(1,1)$ to (N, M) according to the Equation (7). Figure 1(b) indicates the two artificial signals aligned by DTW, it can be seen that the two signals are matched to each other very well based on the optimal warping path produced by dynamic programming. According to the two time series aligned, the accumulated distance matrix has $\mathrm{N} \times \mathrm{M}$ entries. Therefore, the computational complexity of the classic DTW algorithm should be $\mathrm{O}(\mathrm{NM})$ [28].

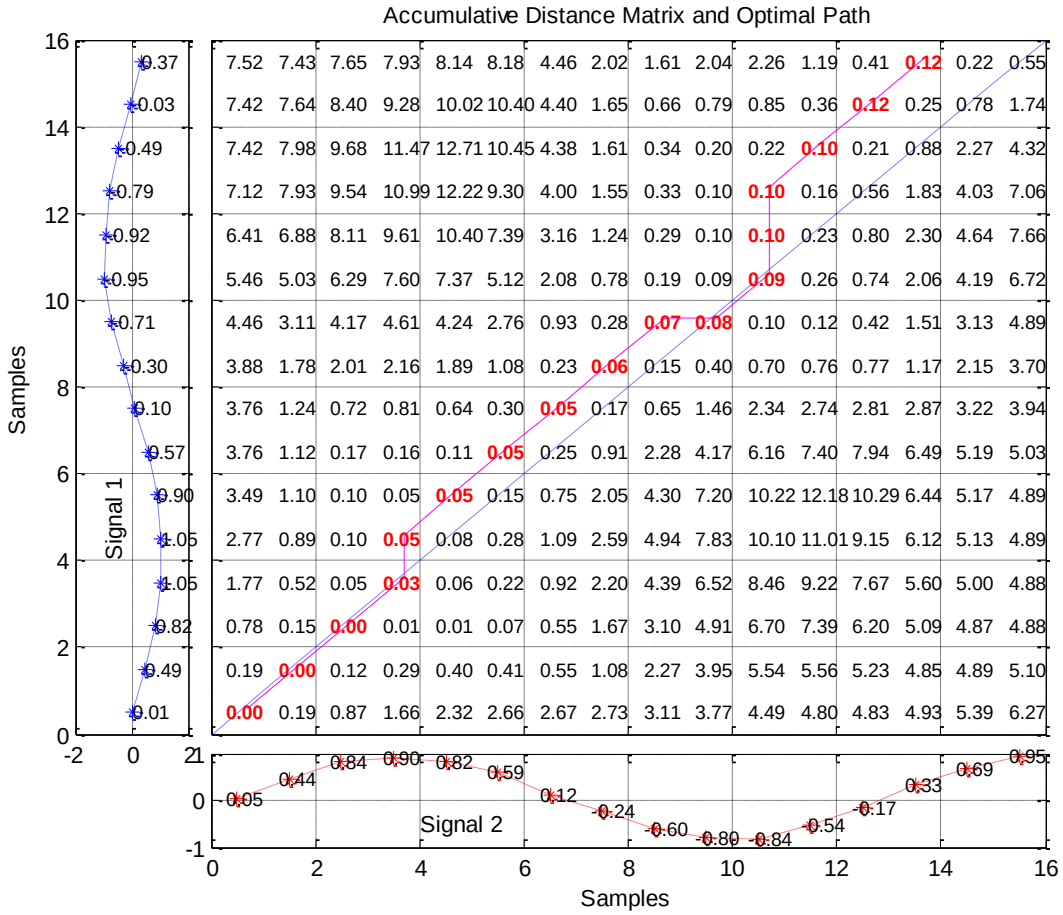

Figure 2 Optimal warping path selected by dynamic programming

3. Phase Current Signal from Reciprocating Compressors

To study the characteristics of the motor stator current signals, the electromagnetic relationships are analyzed in phase A , which is one of the three symmetric phases of a power supply system. If the fundamental frequency of electrical supply is f_s, the instantaneous current signal [4,29,30] under healthy conditions can be expressed as sinusoidal signals:

$$i_A = Icos(2\pi f_s t - \alpha_I) \tag{8}$$

where I denotes the amplitude of the supply current, and α_I is the angular displacement of supply current. Correspondingly, this current interacts with the magnetic flux in motor stator as

$$\emptyset_A = \emptyset cos\,(2\pi f_s t - \alpha_\emptyset) \tag{9}$$

where the amplitude of the magnetic flux is $\emptyset$, and $\alpha_\emptyset$ denotes the angular displacement of magnetic flux. Therefore, the electrical torque produced by the interaction between the current and magnetic flux can be expressed as

$$T = 3P\emptyset I sin\alpha_{\emptyset I} \tag{10}$$

where P is the number of pole pairs, and $\alpha_{\emptyset I} = \alpha_\emptyset - \alpha_I$ is the angular displacement between supply current and magnetic flux. If there is a fault occurring in the rotor system, and supposing the fault generates a sinusoidal wave with a frequency f_F, and the current amplitude and angular

displacement are I_F and α_F respectively. So the additional oscillatory torque can be obtained using Equation (10)

$$\Delta T = 3P\emptyset I_F \sin(2\pi f_F t - \alpha_{\emptyset I} - \alpha_F) \tag{11}$$

This oscillatory torque causes speed fluctuation which can be derived as

$$\Delta\omega = \frac{P}{J}\int \Delta T dt = -\frac{3P^2\emptyset I_F}{4\pi^2 f_F^2 J}\cos(2\pi f_F t - \alpha_{\emptyset I} - \alpha_F) \tag{12}$$

Thus the angular oscillation is:

$$\Delta\alpha_F = \int \Delta\omega dt = \frac{3P^2\emptyset I_F}{4\pi^2 f_F^2 J}\sin(2\pi f_F t - \alpha_{\emptyset I} - \alpha_F) \tag{13}$$

where J is the inertia of the rotor system. And the angular variation in Equation (13) produces phase modulation to the leakage flux. Correspondingly, the magnetic flux in motor stator can be expressed as

$$\emptyset_A^F = \emptyset\cos(2\pi f_s t - \alpha_\emptyset - \Delta\alpha_F) \tag{14}$$

This shows that the flux wave contains nonlinear effects because of the fault in the rotor system. This nonlinear interaction of linkage flux will produce corresponding electromagnetic force and hence induce a nonlinear current signal in the stator [4].

Therefore, referring to the detailed discussion in [4] the simplified stator current can be expressed as

$$i_F = I\cos(2\pi f_s t - \alpha_I) + I_l\cos[2\pi(f_s - f_F)t - \alpha_I - \alpha_F - \varphi] - I_r\cos[2\pi(f_s + f_F)t - 2\alpha_\emptyset + \alpha_I - \alpha_F - \varphi] \tag{15}$$

where φ is the angular displacement of motor equivalent circuit impedance at supply frequency [4], the amplitudes of lower and upper sideband components are denoted by I_l and I_r, respectively. Equation (15) is employed widely for motor condition monitoring. Various fault information can be extracted by analyzing the sideband components of the current signal.

A reciprocating compressor system consists of a typical induction motor, in which the compressor has two basic working processes including compression and expansion. The working process gives rise to a periodically varying load to the driving motor due to the compressor requiring more power in compression than in the expansion [31]. This varying load leads to high oscillation in the measured current signal. According to the Equation (15), the measured current signal can be expressed [4]

$$i_A = I\cos 2\pi f_s t + I_l\cos[2\pi(f_s - f_F)t - \alpha_l] + I_r\cos[2\pi(f_s + f_F)t - \alpha_r] \tag{16}$$

where α_l and α_r denote the angular displacement of the lower and upper sideband components respectively. The sidebands contents of $f_s - f_F$ and $f_s + f_F$ are distributed around the supply frequency content of f_s with very low amplitude showing that the electrical current signal has the similar spectral distributions with an amplitude modulation (AM) signal. Nevertheless, the amplitude of the two sideband components will change with the degree of load and speed fluctuations, which means when the load fluctuation increases with the increase of discharge pressures, the amplitude and phase of the sideband components will change accordingly. Figure 3 shows the stator current signals measured from the two-stage compressor under the conditions of healthy and faulty valve leakage.

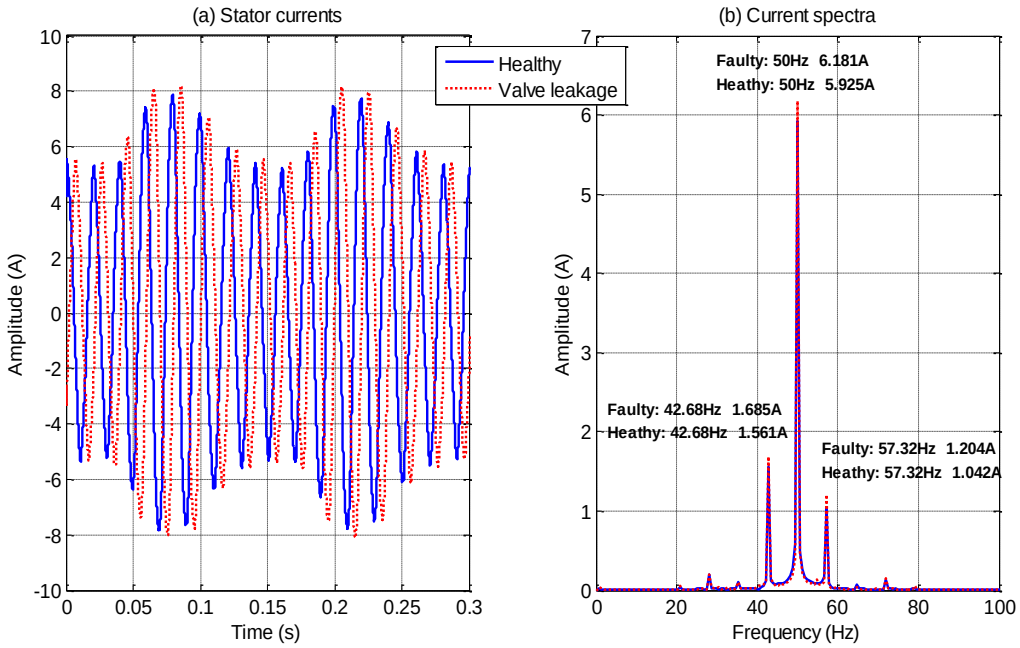

Figure 3 Waveform and spectra of stator current signals from compressor in healthy and faulty valve leakage

It can be seen from Figure 3(a) that the amplitude of the current waveform from the valve leakage is slightly higher than that of the healthy condition and the current signals are modulated by a dynamic load fluctuating according to the waveform. It is also very clear that the two stator currents have similar waveforms but with clear phase shift.

In the spectra, as shown in Figure 3(b), the amplitudes of the supply and sidebands for the valve leakage are also slightly higher than that of the healthy condition, which is consistent with the waveform in Figure 3(a). Therefore, the stator current signals contain useful information for compressor fault detection. The carrier frequency components at the supply frequency 50Hz have high amplitudes and the sideband components at about 50±7.3Hz are also very clear. According to the working frequency of the compressor, the load fluctuating frequency is at 7.3Hz. As discussed in [29, 30], the upper sideband component results from the lower sideband component due to a nonlinear effect caused by the interaction of magnetic flux, load and speed fluctuations.

Moreover, the components at 50Hz have a clear spectral leakage due to the limitation of FT analysis. This leakage will lead to an error in estimating the amplitude at 50Hz, which causes more difficulties in identifying and quantifying the small sidebands which are the main feature used for fault diagnosis.

4. DTW based Fault Detection

According to the theoretical analysis in Section 3, the electrical current signal can be considered as an amplitude modulation (AM) signal. The carrier signal is the supply frequency component at about 50Hz and the load fluctuating component is at about 7.3Hz which is corresponding to the working speed of the compressor and its higher order harmonics. To separate the fluctuating component from the supply components as accurately as possible, a DTW based approach to data processing and fault detection requires including the data manipulation steps shown in Figure 4. It consists of mainly data pre-processing, DTW implementation and detection feature setup.

4.1 Data Pre-processing

The purposes of data pre-processing is to suppress noise, to generate a reference signal and to determine the sliding window length. A low-pass filtering is applied to the raw signal to suppress the inevitable noise. The cut-off frequency of the low pass filter is set to 120Hz so that it removes both the high order harmonics of supply frequency and any random noise originating from measurement and power supply system. This will ensure that the DTW and frequency estimations can be implemented reliably.

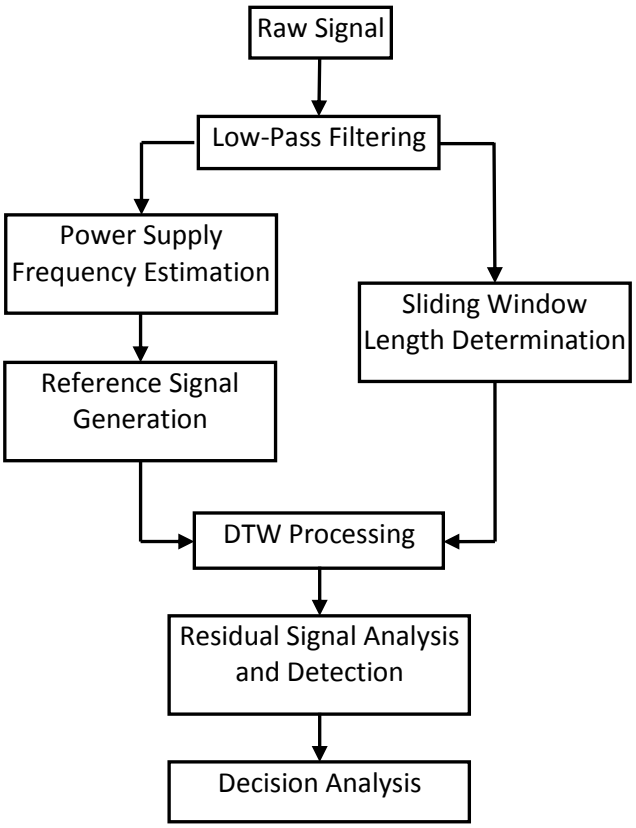

Figure 4 A flow diagram of the proposed data analysis

The reference signal is a sinusoidal signal with the frequency and amplitude calculated from the filtered raw signal. Supposing that the filtered raw signal is $\{x_1, x_2, \cdots, x_n\}$, the amplitude of the reference signal is the amplitude of the filtered raw signal estimated by

$$A_{ref} = \sqrt{2}\sqrt{\frac{1}{n}\sum_n x_n^2} \tag{17}$$

The frequency is estimated by the well-known zero-across detection method [32]. It finds the zero crossing points in a predetermined time interval and counts the number of cycles m that occur in the time interval to obtain the frequency estimation as equation (18). In this study, the length of the measured raw signal is 50,000 and sampling frequency is 24.3 kHz, which means the frequency resolution is 0.486 and it is sufficient for the frequency estimation. In addition, a low-pass filter is used to restrict the bandwidth to the frequencies close to the supply frequency for accurate estimation. However, if the frequency estimation is inaccurate, it will affect the suppression of the supply frequency and hence lead to inaccurate dissimilarities extraction in DTW process for fault detection and diagnostic.

$$f_{ref} = Fs/m \tag{18}$$

where Fs is the sampling frequency. Thus the reference signal can be generated by

$$x_{ref} = A_{ref} cos(2\pi f_{ref} t) \tag{19}$$

However, the phases of measured signals are arbitrary. To implement DTW more efficiently and achieve more accurate results, an initial phase needs to be estimated for a preliminary alignment between the reference signal and the filtered raw signal. In this work, a phase matching approach is developed for initial phase estimation. It uses the Euclidean distance to measure the differences between the reference signal given by Equation (19) at different phases θ and the original filtered raw signal in one cycle. As the phase θ varies from 0 to 2π in a step of about 0.02 rad, the Euclidean distance can be calculated by

$$E_j = \sqrt{\sum_{i=0}^{n} [s_i - x_{refi}(\theta_j)]^2} \; where \; j = 1,2,\cdots,N \tag{20}$$

where, s denotes the filtered raw signal, x_{ref} is the reference signal with a certain phase shift θ_j, and n is the number of the signal points. E should have N elements according to the increase of the phase θ, where N is the number of varies θ. Therefore, each phase angle θ_j corresponds to one Euclidean distance E_j in the vector$E$. The initial phase of the reference signal can be selected by finding the phase angle θ_e which corresponds to the minimized Euclidean distance in the vector$E$.

$$E = \{E_1, E_2, \cdots, E_j, \cdots, E_N\} \text{ Subject to } \theta = \{\theta_1, \theta_2, \cdots, \theta_j, \cdots \theta_N\} \tag{21}$$

$$[E_{min}, \theta_e] = min(E) \tag{22}$$

Thus the reference signal can be regenerated by Equation (19) to have a minimal phase with the filtered raw signal

$$x_{ref} = A_{ref} cos(2\pi f_{ref} t + \theta_e) \tag{23}$$

Similarly, the estimation of the minimum length of the sliding window for DTW processing can be found by calculating the load fluctuating components which correspond to the working speed of the compressor.

$$Lmin = Fs/f_c \tag{24}$$

where f_c is the operating frequency of the compressor. It can be can be calculated by equation (25).

$$f_c = n/60R \tag{25}$$

where n is the speed of compressor in rpm, and R is the transmission ratio. The actual length of the sliding window may be several times of the minimal length depending on data processing tasks. For benchmarking proposed methods with FT based methods, the length is set to 3 times that of the minimum so that the FT based results can have a sufficient resolution for sideband extraction in the Frequency domain.

In addition, to align the reference signal and the filtered raw data with each other, the length of the reference signal should be the same as the length of the sliding window for high efficiency in DTW implementation and memory allocation.

4.2 DTW Implementation

Having produced the reference signal and determined the length of the sliding window, the DTW algorithm can be applied to process the reference signal and the raw signal selected frame by frame. The two signals are matched in the time domain after being processed by DTW, and hence a residual

signal can be obtained by subtracting the raw signal by the reference signal after processing, so that the residual signal can be employed to indicate the dissimilarity between the filtered raw signal and the reference signal. The window is sliding along the raw signal. Therefore, the DTW can be carried out in each sliding window to reveal the differences between the raw signal and reference signal.

Figure 5 shows the interim results of DTW processing at each key step in a typical sliding window. In Figure 5(a) the measured signals are presented with an initial phase when the data is collected where the reference signals are presented at 0 initial phase. Obviously, these two signals are shifted from each other greatly and cannot be compared directly. Figure 5(b) shows the result after a phase shift on the reference signal through the initial phase matching. It can be seen that the overall waveforms are aligned better, but many detailed portions in the waveform are still not matched sufficiently well for comparison. After DTW processing, the raw signal and reference signal are matched to their optimal as shown in Figure 5 (c) and hence the dissimilarity can be revealed by subtracting each other. Figure 5(d) shows the residual signal obtained by the subtraction. Clearly, the residual signal highlights that the major differences between the waveforms shown in Figure 5(a) are around the peak portion of the amplitude modulation when the motor is applied by a higher load during the compression process, which has greater effects of mechanical process as addressed in section 3. Because of this signal enhancement, a more accurate feature can be calculated from this residual signal for fault diagnosis.

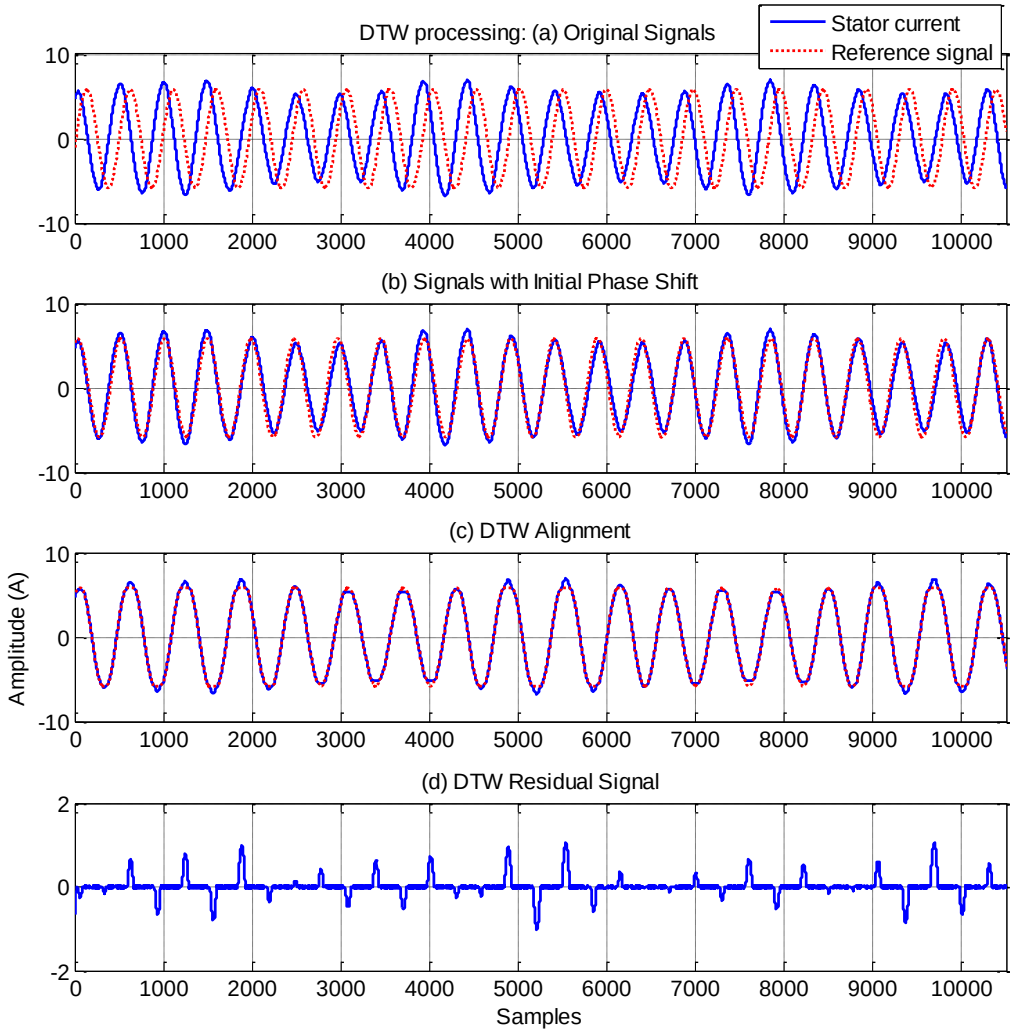

Figure 5 DTW processing data

4.3 Detection Feature

As shown in Figure 4, the final step in the proposed approach is the detection implementation. The aim of applying DTW to process signal is to reveal the differences between the two signals, and the distinction is demonstrated by the residual signal. Therefore, the detection can be made through analysing the residual signal. In the proposed method, the RMS values of the residual signal are employed to measure the amplitude of the residual signals. Compared with peak values, the RMS values produce a more reliable feature when the form of AM modulation varies with different operating conditions and fault cases. Obviously, a higher RMS value indicates a larger difference between the reference signal and the measured signal and hence it indicates the degree of deviation of the signal from sinusoidal due to the modulation effects under compressor conditions.

5. Experimental Evaluation

To examine the performance of the proposed DTW approach in fault detection and diagnosis, a set of electrical current signals are collected from a two-stage reciprocating compressor induced with a number of common faults. The signals are then processed by the DTW approach to produce fault detection and diagnosis results. In addition, the results are also compared with that from traditional FT analysis.

5.1 Compressor Fault Cases

The reciprocating compressor has a common two-stage construction which allows air to be compressed as high as 10bar. It is driven by a 2.5kw three-phase four-pole induction motor through a V-belt with a transmission ratio of 3.2. During the tests, the compressor is induced with three common faults: discharge valve leakage, transmission belt looseness and inter-cooler leakage. These faults lead to low operating efficiency and potential damage to the compressors. The leakage is usually caused by thermal impacts and mechanical vibrations and the belt looseness is a typical feature. The texture of the belt also has some damage. The three types of faults are induced individually to the compressor in order to evaluate the effectiveness of the proposed method in detecting these faults. The valve leakage is produced by drilling a 1mm hole in the discharge valve plate. The distance between two belt pulleys is reduced by 2mm for belt looseness. The case of intercooler leakage is induced by adjusting the tightness of the connecting bolt for the degree of leakage, which is often a consequence of the resonance of the connection line.

During the tests, the current in phase A is measured by a hall effect based current transducer of frequency response from DC to 1.5 kHz. The current signal is then collected by a high speed ADC system at a resolution of 16bit. For each fault the data is collected at 6 different discharge pressures: 4.8bar, 5.5bar, 6.2bar, 6.9bar, 7.6bar and 8.3bar, which covers the operating pressure range specified by the manufacturer. Each collection is 50,000 points which is more than 2 seconds in duration for a sampling rate of 24.3 kHz. This data length covers about 12 compressor cycles which is sufficient for random noise suppression in an average process. In addition, the high sampling rate allows a high accuracy to be obtained in waveform parameter calculation.

5.2 RMS Linear Classifiers

Using the DTW approach in section 4, the raw current signals are processed to obtain residual signals respective to each case and operating pressures. During the processing the sliding window is set to 10500 points in length so that it includes 3 compressor cycles, which allows sufficiently good frequency resolution in DFT based analysis in comparison study. Figure 6 presents a typical residual signal obtained by DTW for the four compressor faulty cases. Comparing the waveform of residual current signals under different conditions has found that the amplitude of the residual signals' waveform varies with the different kinds of the faults. In particular, the valve leakage causes higher amplitudes in the residual signal whereas the intercooler and belt looseness result in lower

amplitude. These are consistent with the changes of modulation characteristics arising from the effect of fault induced load oscillation on the electric current consumption addressed earlier in [5].

To quantify these differences for separating these faulty cases, RMS values of residual signals are calculated for all the cases. Figure 7 shows the RMS of residual signals at different discharge pressures. It is clear that the RMS values of the residual current signals change with the degree of load oscillation. When the compressor operates at a special discharge pressure, such as 6.2bar, the RMS values of the residual signals are also changing with the different kinds of fault cases. It can be seen that the RMS value of the residual signal under the fault of valve leakage is higher than that of the healthy condition and the RMS value of the residual signal under the fault of belt looseness is the lowest in the four conditions. Moreover, when the discharge pressures increase, the RMS values of the residual signals are increasing accordingly under each kind of the fault cases. This means that if there is a fault in the compressor, the load fluctuation characteristic will be altered and hence the RMS values and its distinction will be different from that when the compressor is healthy with the increase of the discharge pressures. Based on this analysis, the faults can be detected and diagnosed by an RMS linear classifier in association with the discharge pressures.

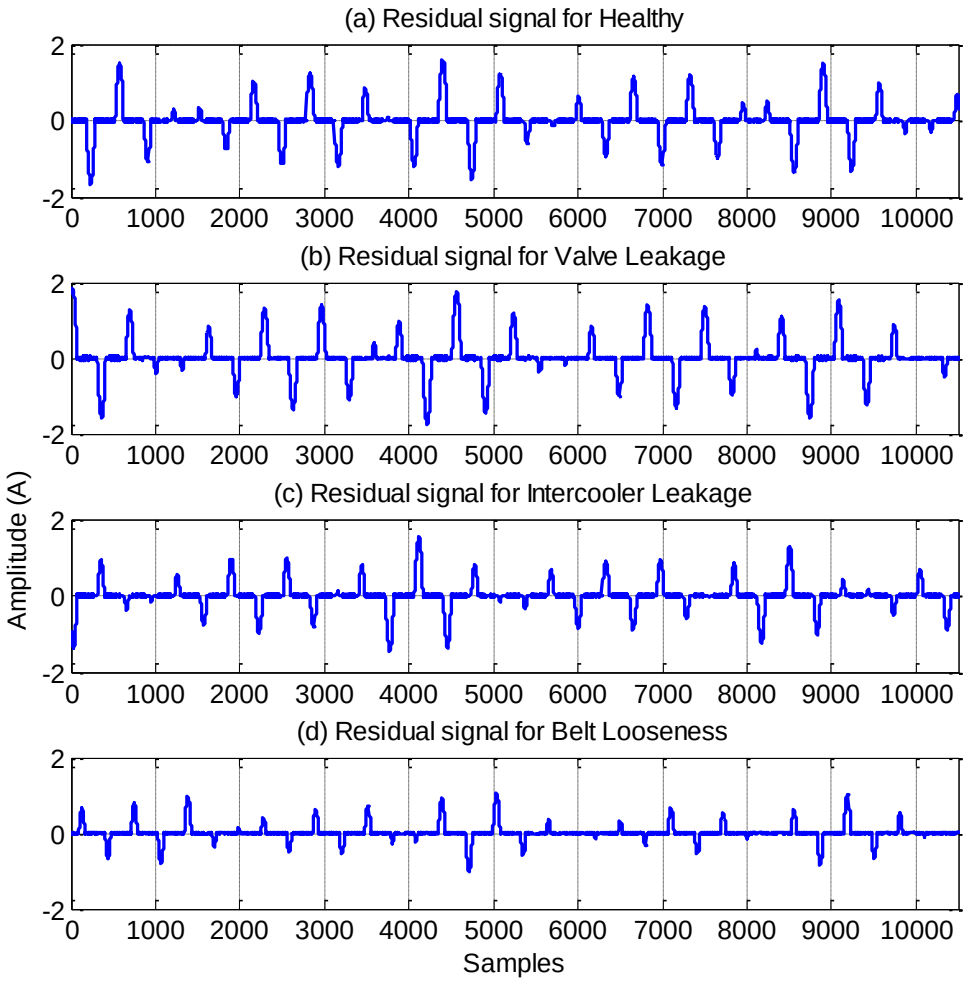

Figure 6 Waveform of residual signals for faulty cases in one sliding window

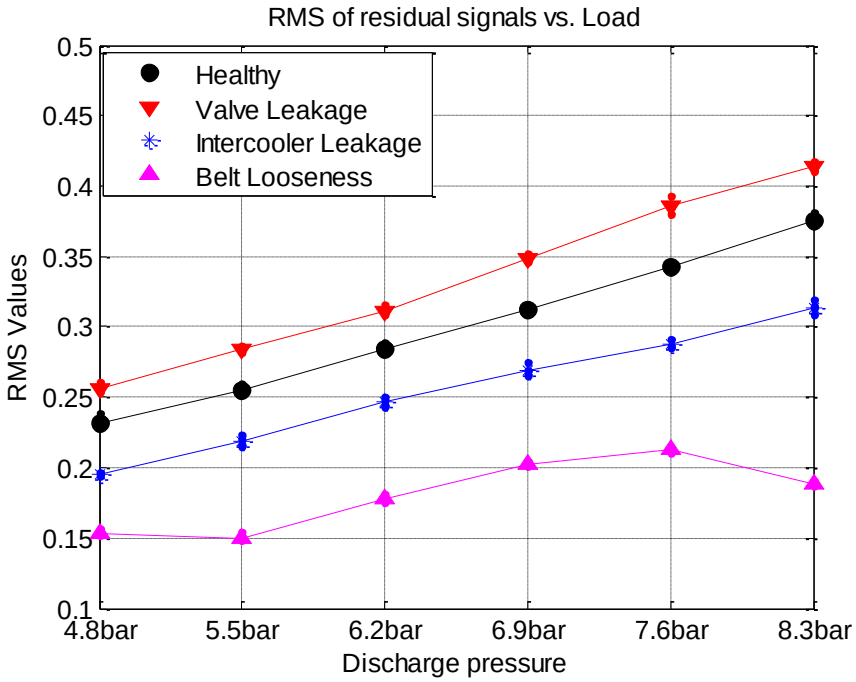

Figure 7 DTW residual signal based detection and diagnosis

5.3 Comparison with FT Based Analysis

To benchmark the performance of the proposed method, the modulation characteristics of the current signals are analysed by two conventional methods: FT based spectrum technique which leads to a sideband amplitude as detection feature, and Hilbert transform analysis which produces an envelope level as the detection feature.

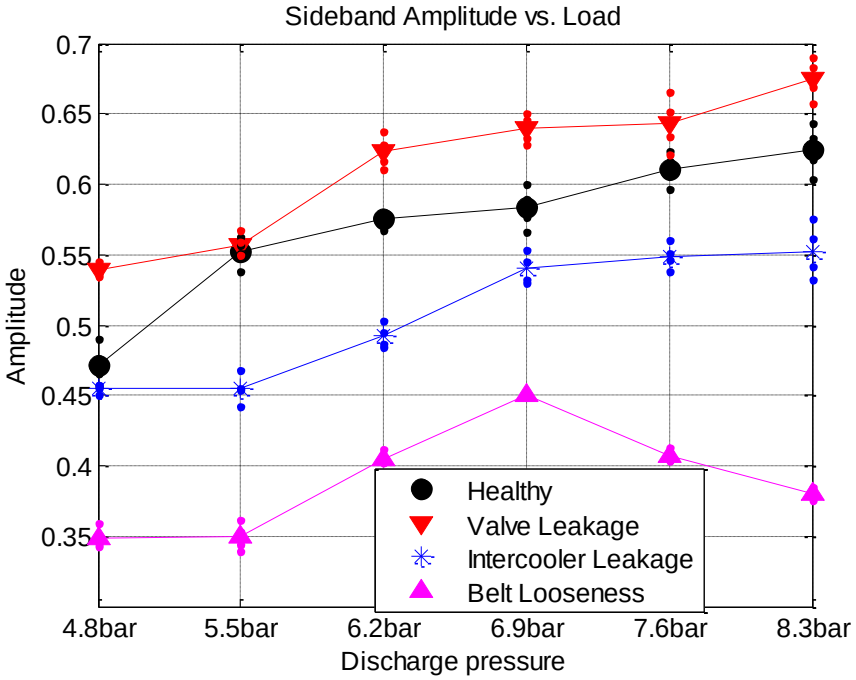

Figure 8 Spectrum sideband based detection and diagnosis

In performing FT calculation a Hanning window is used to reduce the spectral leakage effects. Figure 8 shows the results from the spectrum analysis technique. The feature extraction is carried out by extracting the spectral peak values of the sideband components which are used to reveal the

differences between different operating conditions. It can be seen that the sideband amplitude is unable to produce full separation results between different fault cases under various loads.

In calculating the envelope, a low-pass filter with cut-off frequency of 120Hz is applied to the raw signal and then an FT based Hilbert transform method is used to obtain the envelope signals. Figure 9 shows the RMS values of envelope signals for different fault cases under the different operating discharge pressures. It shows that the envelope analysis can also allow a full separation between the fault cases under the operating conditions of interest. The overall trend is very similar to that of DTW results, demonstrating that DTW is able to capture the modulation characteristics with high accuracy. However, as the envelope RMS values are calculated in the time domain, spectrum leakage etc may be minimised in the time domain envelope signals.

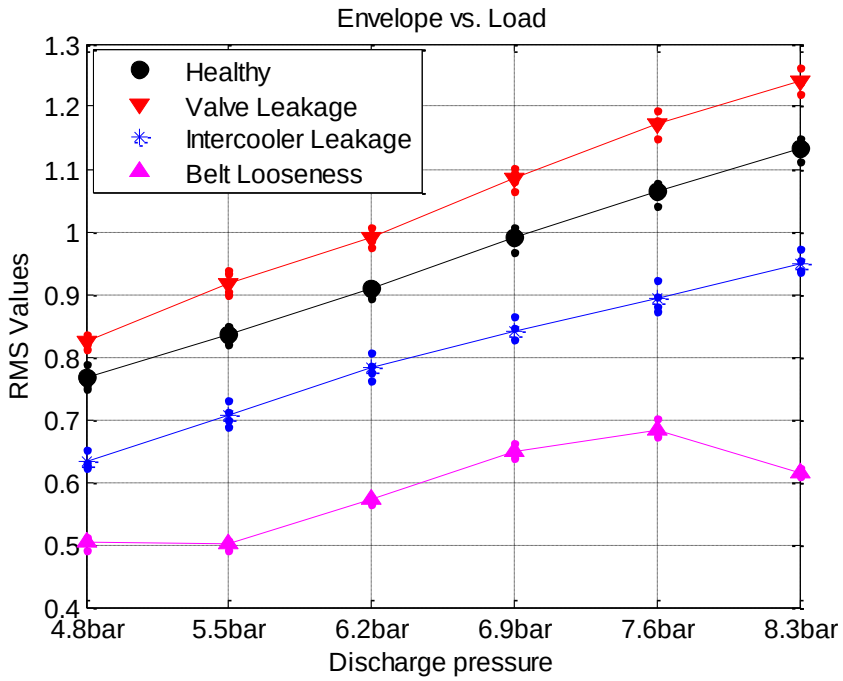

Figure 9 Envelope signal based detection and diagnosis

A careful comparison of Figure 9 and Figure 7 may also find that the deviation of envelope signal RMS values is slightly wider than that of DTW residual RMS values. To make a detailed study, the relative standard deviation (RSD) at each pressure setting for different methods are calculated by

$$RSD = \frac{1}{\bar{x}}\sqrt{\frac{1}{N}\sum_{i=1}^{N}(x_i - \bar{x})^2} \tag{26}$$

where x_i is the RMS value for i^{th} data segment; $\bar{x}$ is the average RMS over different data segments and N is the total segment number. The division of average RMS in equation (26) removes the influences of pressures on RMS and a comparison of deviations between different methods at each pressure can be compared more accurately. Figure 10 shows RSD values for the three methods under different pressures. It was found that the standard deviation for DTW is the smallest, compared with the other two methods. It shows that DTW is less noise sensitive to noise influences and able to produce repeatable results. It also means that the DTW method can differentiate smaller changes for earlier fault detection and diagnosis. Therefore, DTW may produce more accurate and reliable diagnostic results.

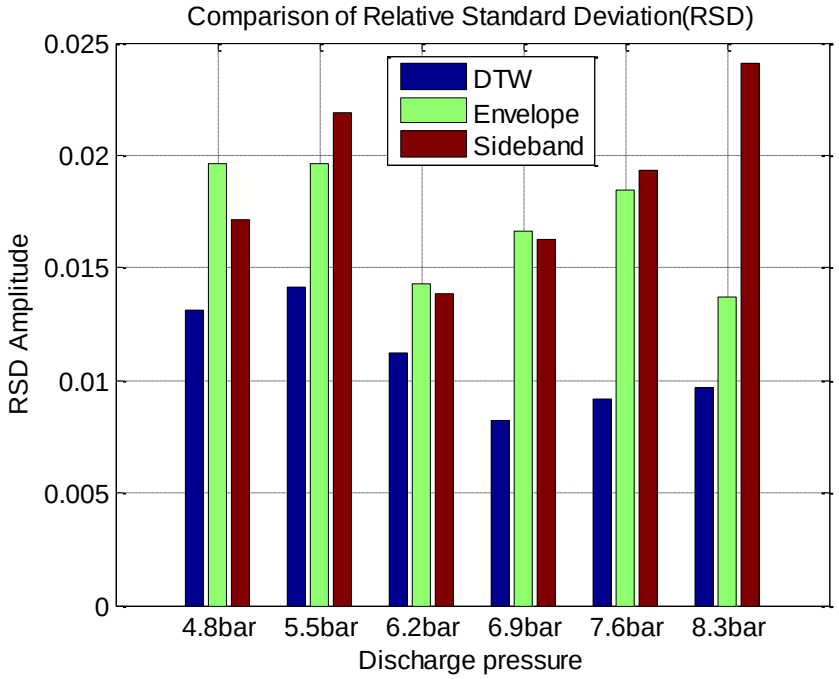

Figure 10 Comparison of standard deviation of three analysis techniques

6. Conclusion

This work concluded that the analysis of electrical current signals based on the DTW has the significant potential to extract weak signals and hence to identify the presence of incipient faults of the downstream mechanical equipment of motor drives. Experiment evaluation is carried out based on a two-stage reciprocating compressor which can lead to significant modulations to motor current signals due to its reciprocating motions and fault conditions. Results show that the sideband components due to modulations can be extracted accurately by the DTW through the introduction of a reference signal of the same frequency contents with the supply power, which result in a residual signal that contains mainly the sideband contents for measuring the modulation levels. The RMS value of residual signal is then used as a feature to detect and diagnose common compressors faults: discharge valve leakage, transmission belt looseness and inter-cooler leakage. The correct diagnosis of these faults over wider operating conditions has demonstrated that the DTW based method is an effective way to obtain accurate features from motor current signals for monitoring the conditions and diagnosing common faults of downstream compressors. Comparatively, the accuracy and reliability of detection and classification from FT spectrum and envelope analysis are slightly lower in differentiating fault cases. In addition, the DTW processing procedure is implemented entirely in the time domain which is easier to be applied in real-time monitoring processes.

References

[1] M.E.H. Benbouzid, A Review of Induction Motors Signature Analysis as a Medium for Faults Detection, IEEE Transactions on Industrial Electronics, VOL. 47, No. 5, October 2000, pp. 984-993.

[2] J. R. Stack, R. G. Habetler and R. G. Harley, Bearing fault detection via autoregressive stator current modeling, Industry Applications Conference, 2003, 38th IAS Annual Meeting.

[3] R. R. Obaid, T. G. Habetler, R. M. Tallam, Detecting load unbalance and shaft misalignment using stator current in inverter-driven induction motors, IEEE int. Elec. Mach. And Drives Conf., 2003, pp. 1454-1458.

[4] F. Gu, Y. M. Shao, A. Naid and A.D. Ball, Electrical motor current signal analysis using a modified bispectrum for fault diagnosis of downstream mechanical equipment, Mechanical Systems and Signal Processing, 25 (1), 2011, pp. 360-372.

[5] M. T. Chen, Digital algorithms for measurement of voltage flicker, Generation, Transmission and Distribution, IEE Proceedings, vol.144, no.2, pp.175-180, Mar 1997.

[6] Fusheng Zhang, Zhongxing Geng, Wei Yuan, The algorithm of interpolating windowed FFT for harmonic analysis of electric power system, Power Delivery, IEEE Transactions on , vol.16, no.2, pp.160-164, Apr 2001

[7] D. Lyon, The Discrete Fourier Transform, Part 4: Spectral Leakage, Journal of Object Technology. Vol. 8, No. 7, 2009.

[8] Yan Feng Li, Kui Fu Chen, Eliminating the picket fence effect of the fast Fourier transform, Computer Physics Communications, Volume 178, Issue 7, 1 April 2008, Pages 486-491.

[9] G. Dalpiaz, A. Rivola, and R. Rubini, Effectiveness and Sensitivity of Vibration Processing Techniques For Local Fault Detection in Gears, Mechanical Systems and Signal Processing, Volume 14, Issue 3, May 2000, Pages 387-412.

[10] C. Myers, L. Rabiner, and A. Rosenberg, Performance tradeoffs in dynamic time warping algorithms for isolated word recognition, IEEE Transactions on Acoustics, Speech, and Signal Processing, vol. 28, no. 6, 1980, pp. 623-635.

[11] H. Sakoe and S. Chiba, Dynamic programming algorithm optimization for spoken word recognition, Acoustics, Speech and Signal Processing, IEEE Transactions on, vol. 26, no. 1, 1978, pp. 43-49.

[12] D. Zhen, J. Gu, T. Wang, F.S. Gu and A.D. Ball, Diagnostic Feature Development based on Dynamic Time Warping of Dynamic Signals under Variable Machine Operating Condition, The Seventh International Conference on Condition Monitoring and Machinery Failure Prevention Technologies, 22-24 June 2010, Stratford-upon-Avon, UK.

[13] E. Keogh and M. Pazzani, Derivative Dynamic Time Warping, In Proc. of the First Intl. SIAM Intl. Conf. on Data Mining, Chicago, Illinois, 2001.

[14] R. Bellman and R. Kalaba, On adaptive control processes, Automatic Control, IRE Transactions on, vol. 4, no. 2, 1959, pp. 1-9.

[15] V.M Velichko, NG Zagoruyko, Automatic Recognition of 200 Words, International Journal of Man-Machine Studies, 2, 223-234, 1970.

[16] H. Sakoe, S. Chiba, A Dynamic Programming Approach to Continuous Speech Recognition, In Proceedings of the Seventh International Congress on Acoustics, volume 3, 1971, pp. 65-69.

[17] F. Itakura, Minimum prediction residual principle applied to speech recognition, IEEE Trans. Acoustics, Speech, and Signal Proc. Vol, 1975. ASSP-23, 52-72.

[18] B. Huang, W. Kinsner, ECG Frame Classification Using Dynamic Time Warping, In W Kinsner, A Sebak, K Ferens (eds.), Proceedings of the Canadian Conference on Electrical and Computer Engineering - IEEE CCECE 2002, volume 2, pp. 1105-1110.IEEE Computer Society, Los Alamitos, CA, USA.

[19] T. Syeda-Mahmood, D. Beymer, F. Wang, Shape-Based Matching of ECG Recordings, In A Dittmar, J Clark, E McAdams, N Lovell (eds.), Engineering in Medicine and Biology Society, 2007. EMBS 2007. 29th Annual International Conference of the IEEE, pp. 2012-2018. IEEE Computer Society, Los Alamitos, CA, USA.

[20] V. Tuzcu, S. Nas,. Dynamic Time Warping as a Novel Tool in Pattern Recognition of ECG Changes in Heart Rhythm Disturbances, In M Jamshidi, M Johnson, P Chen (eds.), Proceedings of the IEEE International Conference on Systems, Man and Cybernetics, volume 1, pp. 182-186 Vol. 1. IEEE Computer Society, Los Alamitos, CA, USA.

[21] J. Aach, GM. Church, Aligning Gene Expression Time Series with Time Warping Algorithms, Bioinformatics, 17(6), 2001, pp. 495-508.

[22] F. Hermans, E. Tsiporkova, Merging Microarray Cell Synchronization Experiments Through Curve Alignment, Bioinformatics, 23(2), 2007, pp. 64-70.

[23] M. Faundez-Zanuy, On-Line Signature Recognition Based on VQ-DTW, Pattern Recognition, 40(3), 2007, pp. 981-992.

[24] TM. Rath, R. Manmatha, Word Image Matching Using Dynamic Time Warping, In R Manmatha (ed.), Proceedings of the IEEE Computer Society Conference on Computer Vision and Pattern Recognition, 2003, volume 2, pp. II-521-II-527. IEEE Computer Society, Los Alamitos, CA, USA.

[25] K. Gollmer, C. Posten, Supervision of Bioprocesses Using a Dynamic Time Warping Algorithm. Control Engineering Practice, 4(9), 1996, pp. 1287-1295.

[26] Pavel Senin, Dynamic Time Warping Algorithm Review, Information and Computer Science Department University of Hawaii at Manoa Honolulu, USA, December 2008.

[27] D. Zhen, A. Alibarbar, X. Zhou, F. Gu, and A.D. Ball, Electrical Motor Current Signal Analysis using a Dynamic Time Warping Method for Fault Diagnosis, 2011 J. Phys.: Conf. Ser. 305 012093.

[28] J. B. Kruskall, and M. Liberman, The symmetric time warping algorithm: From continuous to discrete, Time Warps, String Edits and Macromolecules. Addison-Wesley, 1983.

[29] F. Filippetti, G. Franceschini and C. Tassoni, AI techniques in induction machines diagnosis including the speed ripple effect, IEEE Transactions on Industry Applications, Vol. 34, No. 1, 1998, pp 98-108.

[30] A. Bellini, F. Filippetti, G. Franceschini, C. Tassoni, and G.B. Kliman, Quantitative evaluation of induction motor broken bars by means of electrical signature analysis, IEEE Transactions on Industry Applications, Vol. 37, No. 5, 2001, pp 1248-1255.

[31] R. Schoen, T. Habetler, Motor bearing damage detection using stator current monitoring, IEEE transaction on Industry application vol. 3 No. 6, November/Dec. 1995.

[32] R.W. Wall, Simple methods for detecting zero crossing, Industrial Electronics Society, 2003. IECON '03. The 29th Annual Conference of the IEEE , vol.3, no., pp. 2477- 2481 Vol.3, 2-6 Nov. 2003.